ISBN: 978-3-95450-227-1 ISSN: 2673-5490 doi:10.18429/JACoW-IPAC2022-MOPOTK006

OFF-ENERGY OPERATION FOR THE ESRF-EBS STORAGE RING

L. Hoummi*, T. Brochard, N. Carmignani, L.R. Carver, J. Chavanne, S.M. Liuzzo, T. Perron, R. Versteegen, S. White, ESRF, Grenoble, France
P. Raimondi, SLAC, Menlo Park, California, USA

Abstract

The ESRF-EBS is the first 4th generation source making use of the Hybrid Multi-Bend Achromat (HMBA) lattice cell [1], reaching an equilibrium horizontal emittance of 140 pm.rad in user mode (insertion devices (ID) gaps open). The injection in the storage ring (SR) is conducted with a short booster, operated off-energy. The RF frequency is increased compared to the nominal one to put the beam on a dispersive orbit, thus going off-axis in quadrupoles. The induced dipolar feed down effects reduce the booster horizontal emittance [2, 3].

The same strategy is extended to the ESRF-EBS SR, for an expected emittance reduction of about 20 pm rad. A first approach shifts the RF frequency by +300 Hz to operate at -1% energy offset. Optimal quadrupole and sextupole settings are defined for this off-energy operation based on simulations. The settings are then tested in the SR in terms of dynamic aperture and injection efficiency.

INTRODUCTION

The ESRF-EBS SR provides a 6 GeV electron beam of low equilibrium emittance of 140 pm.rad (insertion devices (ID) gaps open) to 44 beamlines, with canted cells and the inclusion of bending magnet (BM) sources [4] since the end of its commissioning in 2020 [5, 6]. Further reduction of its equilibrium emittance may be achieved by operating on a dispersive orbit, by going off-axis in high-gradient quadrupoles. To do so, the RF frequency is shifted by about 300 Hz, according to:

$$\delta = \frac{\Delta p}{p} = -\frac{1}{\alpha_C}\frac{\Delta f_{RF}}{f_0} \tag{1}$$

with f_0 the synchronous frequency, Δf_{RF} the frequency shift and $\alpha_C = 8.62 \times 10^{-5}$ the momentum compaction factor, under the assumption that it varies slowly with the momentum.

The emittance reduction was first tested on the ESRF-EBS storage ring, by varying its RF frequency within ±500 Hz. No correction was done on the optics. Figure 1 illustrates the variation of the horizontal emittance and the energy spread for different RF frequency shifts. A reduction of about 20 pm rad can be achieved with a RF shift of 300 Hz, which corresponds to about -1% energy deviation, and could increase the photon beam brilliance by about 5-15%.

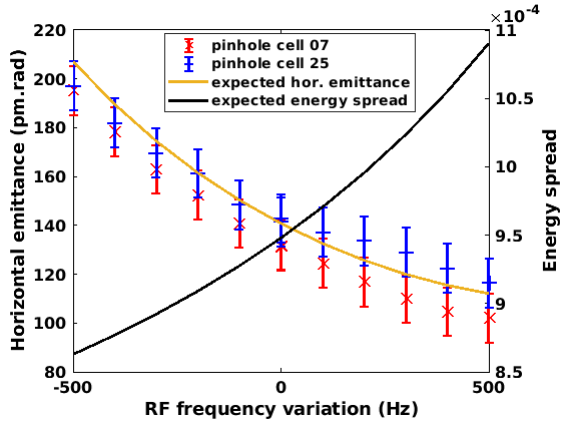

Figure 1: Expected and measured variations of the equilibrium horizontal emittance and energy spread with RF frequency shift, without optics correction.

OFF-ENERGY LATTICE OPTION FOR ESRF-EBS

The RF frequency shift introduces off-axis orbit in the quadrupoles and the sextupoles. This yields to an additional quadrupolar effect in the sextupoles,

$$k_1^{sext} = 2k_2 D_x \delta \tag{2}$$

with k_2 the sextupole strength and D_x the dispersion at the sextupole. This effect introduces beta functions and dispersion modulations that are detrimental in terms of lifetime and injection efficiency. For simplicity, the on-energy optics parameters were taken as a reference for good performances. As such, the off-energy optics were matched to the on-energy ones. Figure 2 compares the Twiss functions and dispersion of the nominal optics and its off-energy option.

The additional quadrupolar strength in the sextupoles binds the tunes and chromaticity corrections and could be compensated using the nearby quadrupoles. Nevertheless, such compensation removes two knobs from the optics matching, required to match the $-I$ transformation between sextupoles. To conserve the tunes and keep chromaticities higher than (6,6) for operation, the sextupole were included in the matching of the optics of the standard cell. The EBS injection cell [7], 2PW and SB insertions and canted cells [4] are also taken into account in the matching.

Table 1 lists the main parameters of the 6 GeV ESRF-EBS HMBA lattice and its off-energy option. The off-energy optics correction and especially the conservation of the horizontal tune decreased the overall dispersion levels and the momentum compaction factor. From (1), the RF shift corre-

* lina.hoummi@esrf.fr

ISBN: 978-3-95450-227-1 ISSN: 2673-5490 doi:10.18429/JACoW-IPAC2022-MOPOTK006

sponding to -1% energy deviation therefore is 280 Hz for an emittance reduction of 19 pm rad.

Table 1: Main Parameters of the ESRF-EBS Storage Ring Lattice at its Nominal Energy and its Off-energy Version

Energy	6 GeV	5.94 GeV
(Q_x, Q_y)	(76.18, 27.34)	(76.18, 27.34)
Nat. ϵ_x	141 pm.rad	122 pm.rad
α_c	8.62×10^{-5}	7.65×10^{-5}
Chromaticity	(7.0, 6.0)	(6.6, 6.2)
Energy spread	9.5×10^{-4}	1.0×10^{-3}
Energy loss	2.6 MeV	2.5 MeV
RF frequency shift	0 Hz	+280 Hz
β_x at injection	18.5 m	19.0 m

Overall, the off-energy optics require lower quadrupolar strengths. The dipole-quadrupole magnets (DQ) were all varied by -0.5% to recover the cell phase advance and maintain the $-I$ transformation between sextupoles in the standard cells. Variations of other quadrupoles are within ±5% range. Sextupole strengths decreased by close to 2% on average. All variations remain under the power supply tolerances. For sake of simplicity, the injection sextupole were left identical to the standard ones, leaving six knobs for further optimisation.

DYNAMIC APERTURE AND LIFETIME WITH ERRORS

Figure 3 compares the dynamic aperture at the injection point of the nominal lattice and its off-energy optics for both considered energy deviations, 0% and -1% as well as the variation of the momentum acceptance over one standard cell. Particles were tracked over 5000 turns, using Accelerator Toolbox (A.T.) [8]. The off-energy optics recover and exceed the dynamic aperture at the injection point of the nominal lattice, while presenting a 20% reduction in lifetime.

For a fair comparison, the same set of errors was applied on the on-energy and the off-energy optics. Ten lattices including errors and correction were generated on-energy.

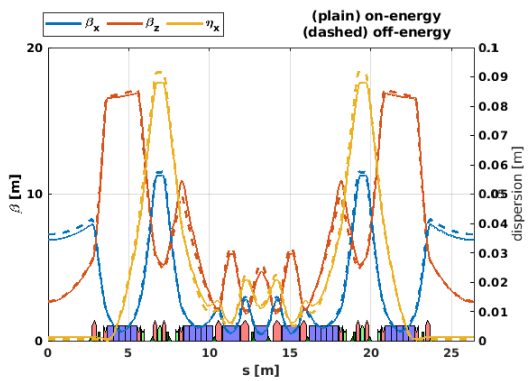

Figure 2: Twiss functions of the standard cell of (plain) the current ESRF-EBS storage ring lattice and (dashed) its off-energy option.

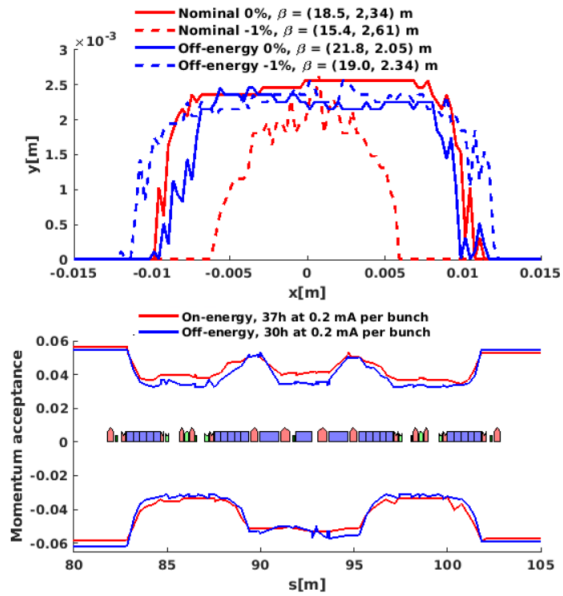

Figure 3: (top) Dynamic aperture and β-functions at the injection point for both energy deviation 0% and -1%, and (bottom) momentum acceptance over one standard cell and Touschek lifetime of the nominal lattice and its off-energy settings.

Then, the modifications on the quadrupoles and sextupoles required to go from the on-energy to the off-energy optics were equally applied to all lattices. The same procedure was used to set the off-energy optics in the SR during machine dedicated time. These ten sets of identical errors and corrections were then used either for on- or off-energy DA and lifetime computations.

Figure 4 compares the DA at injection of the lattices without errors and with error and corrections, for both studied optics. The DA with errors and correction are comparable for both cases, ensuring the conservation of the correction conducted on-energy when transposing to the off-energy optics. The lifetimes were calculated for three operation current per bunch. The results are listed in Table 2.

Table 2: Touschek Lifetime Calculations for Three Currents per Bunch of ESRF-EBS and for Both Considered Lattices with the Same Sets of Errors and Corrections, Assuming $Z_{//} = 0.3\Omega$ and $\epsilon_V = 10$ pm.rad

Current per bunch	On-energy	Off-energy
0.2 mA	37.9 ± 1.3 h	29.9 ± 2.5 h
5.8 mA	2.9± 0.1 h	2.3 ± 0.2 h
10 mA	1.9 ± 0.1 h	1.5 ± 0.1 h

Ongoing injection sextupole optimisation using a mix between Multi-Objective Genetic Algorithm and Particle Swarm Optimisation (MOPSO) aim at increasing the off-energy optics lifetime [9]. As mentioned above, tunes and chromaticity must be corrected simultaneously for the off-energy optics. For MOGA and MOPSO optimisations, two quadrupole families (QF1/QD2) and two sextupole families

ISBN: 978-3-95450-227-1 ISSN: 2673-5490 doi:10.18429/JACoW-IPAC2022-MOPOTK006

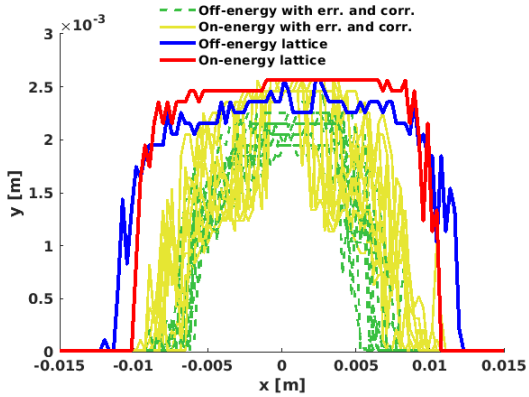

Figure 4: Dynamic aperture at the injection point for the nominal lattice and its off-energy optics with and without errors and corrections.

(SF2/SD1) are used via a 4x4 response matrix to correct the tunes and the chromaticity after changing the injection sextupoles.

EXPERIMENTAL TEST OF THE OFF-ENERGY OPTICS

The off-energy settings were tested on the ESRF-EBS storage ring at low current. For a fair comparison, the nonlinear optimisation of the sextupoles and octupoles were removed from the nominal lattice, as well as closed orbit bumps. The implementation of the off-energy optics was conducted by steps of 50 Hz in RF frequency shift with tunes and orbit correction. The correction kept the on-energy values of the respective tunes and orbit 2×2 response matrices. Then, a corresponding fraction of the optics variation was sent to the quadrupoles and sextupoles. Future tests will assess the improvements introduced by using a complete 4×4 matrix. Injection could be conducted directly on the shifted optics, the injection efficiency reached 35% with no tuning of the injectors.

Linear optics measurements [10] were conducted on the on- and off-energy optics, as well as one set of correction. Beating of the beta-functions and the dispersion were compared with their theoretical model and remain comparable in both cases: $\left(\frac{\Delta\beta}{\beta}\right)$ was $(1.4, 1.3) \pm (1, 1)\%$ and $(1.5, 2.3) \pm (1, 1)\%$ and ΔD_x, 0.66 ± 0.01 mm and 0.97 ± 0.01 mm for the on-energy and off-energy settings respectively. The nominal chromaticities were measured at $(10, 10) \pm (1, 1)$, and $(8.4, 10) \pm (1, 1)$ for the off-energy optics.

The dynamic apertures were measured using one of the collimators [11] and monitoring the particle losses and lifetime. Table 3 lists the obtained results scaled at the injection point. The off-energy optics recover the on-energy DA, which still lacks online optimisation at the level of the on-energy optics [12, 13].

To simulate the user mode, radiation power was generated in the machine by evenly closing the gaps of the insertion devices. The emittance measurements in Fig. 5 were rescaled according to the off-energy optics at the pinholes. During user time, the emitted power typically varies within 80-120 kW. At this power, the measured equilibrium emittance, with no vertical beam blow-up is about 100 pm rad.

Table 3: Dynamic Aperture Measurement Scaled to the Injection Point

Optics	RF shift	Horizontal DA
On-energy	0 Hz	$[-6.5; 6.0] \pm [0.2; 0.2]$ mm
	+280 Hz	$[-5.4; 4.9] \pm [0.2; 0.3]$ mm
Off-energy	0 Hz	$[-5.0; 4.3] \pm [0.2; 0.2]$ mm
	+280 Hz	$[-6.3; 6.0] \pm [0.2; 0.4]$ mm

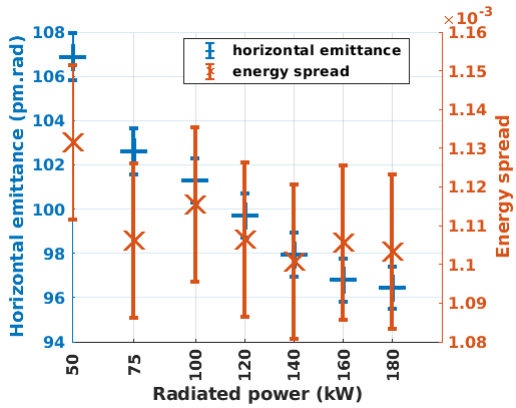

Figure 5: Measured horizontal emittance and energy spread with progressively closed insertion device gaps and their expected radiated power at high current, for the off-energy settings of the ESRF-EBS storage ring.

CONCLUSIONS

Off-energy optics were developed for a reduction in natural horizontal emittance of about 20 pm rad while conserving the magnetic strengths within their power supply tolerances and providing an estimated increase of 5-15% of the photon beam brilliance. Future improvements of the optics will include theoretical sextupole optimisation using the injection sextupoles as well as experimental lifetime optimization [13] at high current. The off-energy optics were successfully implemented in the storage ring, with no change in tune and orbit correction response matrices. Further tests will tune the injectors to follow the reduced SR beam energy and to maximise the injection efficiency.

The off-energy settings induce high closed orbit distortion in the center of the cells, impacting the dipole sources. The beam arrives with a measured angle of about 400 µrad, which would require an adjustment of the front end position by about 8-9 millimeters. The impact of the highest energy spread on the spectrum quality of high-order undulator harmonics is being studied.

ISBN: 978-3-95450-227-1 ISSN: 2673-5490 doi:10.18429/JACoW-IPAC2022-MOPOTK006

REFERENCES

[1] L. Farvacque *et al.*, "A Low-Emittance Lattice for the ESRF", in *Proc. IPAC'13*, Shanghai, China, May 2013, paper MOPEA008, pp. 79–81.

[2] N. Carmignani *et al.*, "Operation Improvements and Emittance Reduction of the ESRF Booster", in *Proc. IPAC'18*, Vancouver, Canada, Apr.-May 2018, pp. 4077–4080. doi:10.18429/JACoW-IPAC2018-THPMF017

[3] N. Carmignani, L. R. Carver, S. M. Liuzzo, T. P. Perron, and S. M. White, "Operation of the ESRF Booster with the New EBS Storage Ring", in *Proc. IPAC'21*, Campinas, Brazil, May 2021, pp. 221–224. doi:10.18429/JACoW-IPAC2021-MOPAB051

[4] S. M. Liuzzo *et al.*, "ESRF-EBS Lattice Model with Canted Beamlines", in *Proc. IPAC'18*, Vancouver, Canada, Apr.-May 2018, pp. 4081–4083. doi:10.18429/JACoW-IPAC2018-THPMF019

[5] P. Raimondi *et al.*, "Commissioning of the hybrid multibend achromat lattice at the European Synchrotron Radiation Facility", *Phys. Rev. Accel. Beams*, vol. 24, p. 110701, 2021. doi:10.1103/PhysRevAccelBeams.24.110701

[6] S. M. White *et al.*, "Commissioning and Restart of ESRF-EBS", in *Proc. IPAC'21*, Campinas, Brazil, May 2021, pp. 1–6. doi:10.18429/JACoW-IPAC2021-MOXA01

[7] S. M. White and T. P. Perron, "Injection Using a Non-Linear Kicker at the ESRF", presented at the IPAC'22, Bangkok, Thailand, Jun. 2022, paper THPOPT040, this conference.

[8] B. Nash *et al.*, "New Functionality for Beam Dynamics in Accelerator Toolbox (AT)", in *Proc. IPAC'15*, Richmond, VA, USA, May 2015, pp. 113–116. doi:10.18429/JACoW-IPAC2015-MOPWA014

[9] X. Huang and J. Safranek, "Nonlinear dynamics optimization with particle swarm and genetic algorithms for SPEAR3 emittance upgrade", *Nucl. Instrum. Methods Phys. Res., Sect. A*, vol. 757, p. 48-53, 2014. doi:10.1016/j.nima.2014.04.078

[10] S. M. Liuzzo *et al.*, "FILO: A New Application to Correct Optics in the ESRF-EBS Storage Ring", presented at the IPAC'22, Bangkok, Thailand, Jun. 2022, paper TUPOMS006, this conference.

[11] R. Versteegen *et al.*, "Collimation scheme for the ESRF Upgrade", in *Proc. IPAC'15*, Richmond, VA, USA, May 2015, pp. 1434–1437. doi:10.18429/JACoW-IPAC2015-TUPWA017

[12] S. M. Liuzzo, N. Carmignani, L. R. Carver, L. Hoummi, T. P. Perron, and S. M. White, "A Long Booster Option for the ESRF-EBS 6 GeV Storage Ring", presented at the IPAC'22, Bangkok, Thailand, Jun. 2022, paper TUPOMS007, this conference.

[13] N. Carmignani *et al.*, "Online Optimization of the EBS Storage Ring Lifetime", presented at the IPAC'22, Bangkok, Thailand, Jun. 2022, paper THPOPT001, this conference.